Scandium-doped aluminum nitride photonic integration platform

Nanxi Li*, Wing Wai Chung, Jia Sheng Goh, Yat Fung Tsang, Landobasa Y. M. Tobing, Chong Pei Ho, Binni Varghese, Leh Woon Lim, Minghua Li, Huamao Lin, Qingxin Zhang, Doris K. T. Ng, Lennon Y. T. Lee, and Xianshu Luo
Institute of Microelectronics, A*STAR (Agency for Science, Technology and Research), 2 Fusionopolis Way, Singapore 138634
*Corresponding Author: linx1@ime.a-star.edu.sg

ABSTRACT

Aluminum nitride (AlN) is a promising photonics material contributed by its wide transparency window and remarkable nonlinear optical property. Moreover, its nonlinear effect can be further enhanced by doping Scandium (Sc). Such nonlinear optical property brings potential for high efficiency in nonlinear optical generation processes, such as 2^{nd} harmonic generation and frequency comb generation. Although the nonlinear optical property of Sc-doped AlN looks promising, its waveguide is facing challenge on loss reduction. In this work, we report Sc-doped AlN photonic integrated circuit with reduced waveguide loss of 6 dB/cm around 1550 nm. The waveguide has Sc doping concentration of 10%. Its etching process is tailored through a design of experiment (DoE) approach to achieve smooth surface. An annealing process is also applied to patterned waveguide for optical loss reduction. A loaded Q of 1.41×10^4 has also been reported from microring resonator on the same wafer. The reported result paves the way towards low-loss Sc-doped AlN for photonic integrated circuits.

Keywords: Integrated optics devices; Integrated optics materials.

1. INTRODUCTION

Aluminum nitride (AlN) is a promising material for photonic integrated circuit (PIC) [1,2]. It has wide transparency window for waveguide to work from ultra-violet to mid-infrared wavelength regime [3,4], significant nonlinear optical effect for nonlinear optical generation [5,6], and piezoelectric effect for photon-phonon interactions [7,8]. Also, it can be fabricated on silicon wafer with low cost using a complementary metal-oxide semiconductor (CMOS)-compatible process [9]. Various functional photonic devices have been demonstrated on AlN, including modulator [10], frequency comb generator [11], parametric oscillator [12], and optical phased array [13]. Furthermore, the nonlinear optical effect and piezoelectric effect of AlN can be further enhanced by doping Scandium (Sc) into it [14,15]. Sc-doped AlN is a common material implemented in micro-electromechanical systems (MEMS) [16–19], contributed by its superior piezoelectric and pyroelectric property. In terms of optical property, the 2^{nd} order nonlinear coefficient of Sc-doped AlN material has been reported an order of magnitude larger than AlN material without doping [14]. Its superior nonlinear optical property is contributed to the increased non-centrosymmetric crystal structure by replacing Al atom with Sc atom in crystal lattice. Such nonlinear optical property brings potential for high efficiency in nonlinear optical generation processes, such as 2^{nd} harmonic generation and frequency comb generation. Although the nonlinear optical property of Sc-doped AlN looks promising, its waveguide is currently facing challenge on loss reduction. Sc-doped AlN waveguide has been recently reported with optical loss of 9 dB/cm around 1550 nm [20]. The reported waveguide has Sc doping concentration of 15% [20]. In addition, when we were writing up this paper, we also found a more recent work reporting Sc-doped AlN microring resonators with Sc concentration of 9% and 18% [21].

In this work, we report 10% Sc-doped AlN PIC with waveguide loss of 6 dB/cm measured around 1550 nm using cut-back method. The waveguide height is 500 nm, with width as design variation ranging from 300 nm to 1000 nm. The waveguide etching process is tailored through a design of experiment (DoE) approach to achieve smooth surface. An annealing process is also applied to patterned waveguide for optical loss reduction. The microring resonator on the same platform demonstrates a loaded Q of 1.41×10^4. The reported result paves the way towards low-loss Sc-doped AlN for PIC, with potential applications in communication, sensing, and quantum computing.

2. SCANDIUM-DOPED ALUMINUM NITRIDE PHOTONIC INTEGRATED CIRCUIT

Our Sc-doped AlN PIC was fabricated on 8-inch Si wafers with 4 µm thick thermal oxide layer on top, using CMOS-compatible fabrication facilities. The fabrication process is similar to our earlier report on AlN photonics platform [9], except that 10% Sc-doped Al target is used during the physical vapor deposition (PVD) process. Furthermore, the dry etching recipe is tailored for 10% Sc-doped AlN thin film to achieve smooth sidewall. In addition, the etching hardmask and photoresist thicknesses are optimized to achieve 400 nm critical dimension for Sc-doped AlN PIC. The fabricated 8-inch wafer is illustrated in the photo image in Fig. 1(a). The cross section of patterned 500-nm thick photonic waveguide is shown in scanning electron microscopy (SEM) image in Fig. 1(b).

2.1 Photonic waveguide

Fig. 1(c) illustrates the electric field intensity distribution of transverse magnetic (TM) mode confined within the waveguide. The optical loss of the waveguide with width of 300 to 400 nm operating in TM mode is measured around 1550 nm using cut-back method. The microscopic image of patterned cut-back structure is shown in Fig. 1(d), with waveguide length variations of 1.86 mm, 7.86 mm, 11.5 mm, 18.3 mm, and 27.3 mm. The total loss of these waveguides with respect to different waveguide lengths is plotted in Fig. 1(e). With linear curve fitting of measured loss, the waveguide loss can be obtained as 6 dB/cm for TM mode around 1550 nm wavelength. More details on the waveguide loss characterization setup can be found in the later section (same setup as microring resonator).

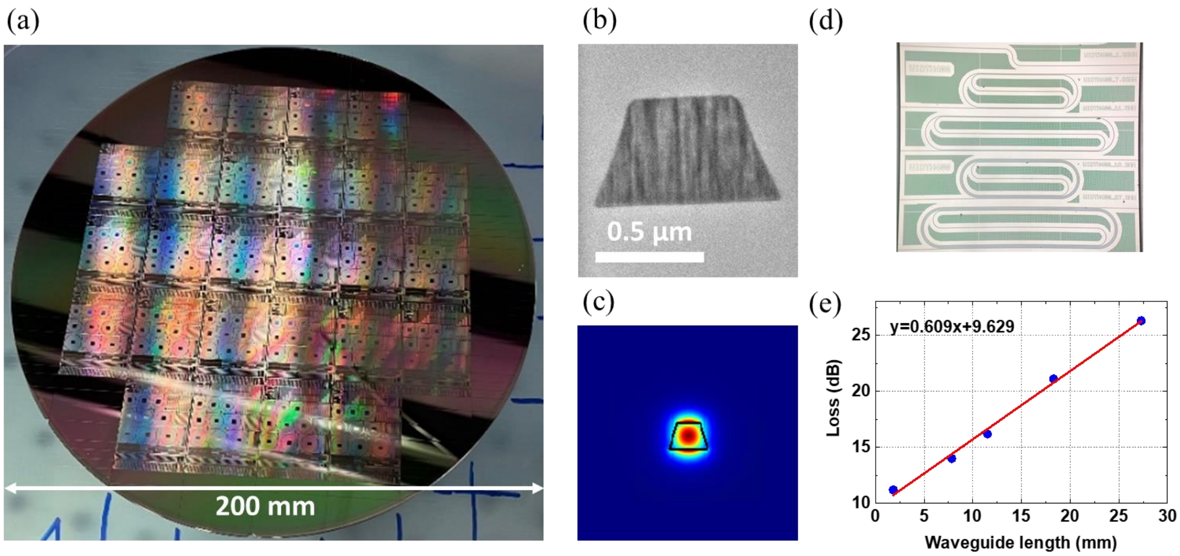

Figure 1. (a) Fabricated 8-inch wafer. (b) Cross sectional SEM image of patterned 500-nm thick photonic waveguide. (c) Electric field intensity distribution of TM mode confined within the waveguide. (d) Patterned cut-back structure with waveguide length variations of 1.86 mm, 7.86 mm, 11.5 mm, 18.3 mm, and 27.3 mm. (e) Plot of measured waveguide loss with respect to waveguide lengths with linear curve fitting indicating the waveguide loss of 6 dB/cm for TM mode around 1550 nm wavelength.

2.2 Microring resonator

Microring resonator is a typical structure in a PIC used as spectrum filter [22,23], modulator [24,25], or nonlinear optical generator [26,27]. Microring resonators have also been patterned in Sc-doped AlN photonics platform, with characterization setup and results presented Fig. 2(a) and 2(b, c), respectively. A tunable laser (Keysight N7776C) cascaded with a polarization controller is used as light source, and a power meter (Keysight N7742C) is used for photodetection. Both are synchronized for wavelength sweeping to capture the passive spectrum response of the microring device. Tapered fibers are used for optical coupling into and out of the device under test (DUT). The microring has a diameter of 120 µm, and waveguide width of 1.2 µm. The microscopic image of the microring is included in the inset in Fig. 2(a). The TM mode passive response of the microring (in dB scale) is shown in Fig. 2(b). One typical resonance is selected and fitted with Lorentzian function, as shown in Fig. 2(c). From the fitted curve, a loaded Q of 1.41×10^4 can be obtained.

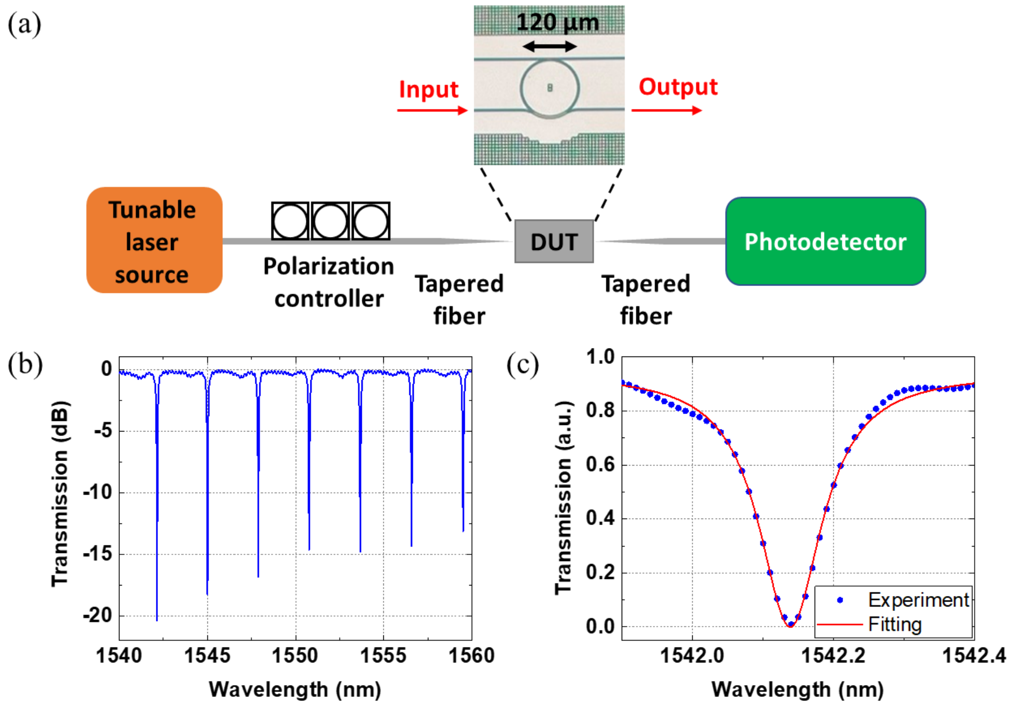

Figure 2. (a) Microring resonators characterization setup includes a tunable laser source (Keysight N7776C) cascaded with a polarization controller as light source for wavelength sweeping, a power meter (Keysight N7742C) for photodetection, and tapered fibers for optical coupling into and out of the device under test (DUT). Inset: the microscopic image of the microring. (b) TM mode passive response of the microring. (c) Typical resonance fitted with Lorentzian curve demonstrating a loaded Q of 1.41×10^4.

3. CONCLUSION

To sum up, a 10% Sc-doped AlN photonic integration platform has been demonstrated on 8-inch Si wafers using CMOS-compatible fabrication facilities. A waveguide loss of 6 dB/cm around 1550 nm is obtained through cut-back structure with waveguide width of 300-400 nm. A microring resonator with a diameter of 120 µm and a loaded Q of 1.41×10^4 has also been reported. The reported result paves the way towards low-loss Sc-doped AlN for PIC with superior nonlinear optical property for nonlinear optical generation.

ACKNOWLEDGEMENTS

This work is supported by Agency for Science, Technology and Research under grant no. C220415015.

REFERENCES

[1] Liu, X., Bruch, A. W. and Tang, H. X., "Aluminum nitride photonic integrated circuits: from piezo-optomechanics to nonlinear optics," Adv. Opt. Photon., **15**(1), 236–317 (2023).

[2] Li, N., Ho, C. P., Zhu, S., Fu, Y. H., Zhu, Y. and Lee, L. Y. T., "Aluminium nitride integrated photonics: a review," Nanophotonics **10**(9), 2347–2387 (2021).

[3] Pernice, W. H. P., Xiong, C., Schuck, C. and Tang, H. X., "Second harmonic generation in phase matched aluminum nitride waveguides and micro-ring resonators," Appl. Phys. Lett. **100**(22), 223501 (2012).

[4] Majkić, A., Puc, U., Franke, A., Kirste, R., Collazo, R., Sitar, Z. and Zgonik, M., "Optical properties of aluminum nitride single crystals in the THz region," Opt. Mater. Express **5**(10), 2106–2111 (2015).

[5] Jung, H., Xiong, C., Fong, K. Y., Zhang, X. and Tang, H. X., "Optical frequency comb generation from aluminum nitride microring resonator," Opt. Lett. **38**(15), 2810–2813 (2013).

[6] Guo, X., Zou, C.-L. and Tang, H. X., "Second-harmonic generation in aluminum nitride microrings with 2500%/W conversion efficiency," Optica **3**(10), 1126–1131 (2016).

[7] Tadesse, S. A. and Li, M., "Sub-optical wavelength acoustic wave modulation of integrated photonic resonators at microwave frequencies," Nat. Commun. **5**(1), 5402 (2014).
[8] Li, H., Tadesse, S. A., Liu, Q. and Li, M., "Nanophotonic cavity optomechanics with propagating acoustic waves at frequencies up to 12 GHz," Optica **2**(9), 826–831 (2015).
[9] Li, N., Ho, C. P., Cao, Y., Zhu, S., Chen, G. F. R., Fu, Y. H., Zhu, Y., Tan, D. T. H. and Lee, L. Y. T., "Aluminum Nitride Photonics Platforms on Silicon Substrate," Conference on Lasers and Electro-Optics, paper STh2H.3, Optical Society of America (2021).
[10] Xiong, C., Pernice, W. H. P. and Tang, H. X., "Low-Loss, Silicon Integrated, Aluminum Nitride Photonic Circuits and Their Use for Electro-Optic Signal Processing," Nano Lett. **12**(7), 3562–3568 (2012).
[11] Bruch, A. W., Liu, X., Gong, Z., Surya, J. B., Li, M., Zou, C.-L. and Tang, H. X., "Pockels soliton microcomb," Nat. Photon. **15**(1), 21–27 (2021).
[12] Bruch, A. W., Liu, X., Surya, J. B., Zou, C.-L. and Tang, H. X., "On-chip χ(2) microring optical parametric oscillator," Optica **6**(10), 1361–1366 (2019).
[13] Li, N., Lim, L. W., Xue, J., Ho, C. P., Zhu, S., Fu, Y. H. and Lee, L. Y. T., "Aluminum Nitride Nanophotonic Phased Array on an 8-inch Silicon Wafer," Conference on Lasers and Electro-Optics, paper AM3M.5, Optica Publishing Group (2023).
[14] Yoshioka, V., Lu, J., Tang, Z., Jin, J., Olsson, R. H. and Zhen, B., "Strongly enhanced second-order optical nonlinearity in CMOS-compatible Al1−xScxN thin films," APL Materials **9**(10), 101104 (2021).
[15] Y. Kusano, I. Ishii, T. Kamiya, A. Teshigahara, G. -L. Luo, and D. A. Horsley., "High-SPL Air-Coupled Piezoelectric Micromachined Ultrasonic Transducers Based on 36% ScAlN Thin-Film," IEEE Trans. Ultrason. Ferroelectr. Freq. Control **66**(9), 1488–1496 (2019).
[16] Xu, L., Ng, D. K. T., Chen, W., Li, N., Ho, C. P., Goh, D. J., Zhang, Y., Zhang, Q. and Lee, L. Y. T., "Low-power contactless button system based on MEMS ScAlN pyroelectric detector," MOEMS and Miniaturized Systems XXII **12434**, 18–23, SPIE (2023).
[17] Colombo, L., Kochhar, A., Xu, C., Piazza, G., Mishin, S. and Oshmyansky, Y., "Investigation of 20% scandium-doped aluminum nitride films for MEMS laterally vibrating resonators," 2017 IEEE International Ultrasonics Symposium (IUS), 1–4 (2017).
[18] Cai, H., Khairy, M. H., Ang, R. C. F., Xu, L., Ng, D. K. T., Li, N., Gu, Z., Kong, A., Chen, W., Seit, W. W., Ching, E. W. L., Jaafar, N., Wang, H., Tobing, L. Y. M., Lim, L. W., Zhang, Q. and Lee, L. Y. T., "On-chip CO2 sensor integrated with MEMS emitter and pyroelectric detector," Silicon Photonics XVIII **12426**, 103–107, SPIE (2023).
[19] Su, J., Niekiel, F., Fichtner, S., Thormaehlen, L., Kirchhof, C., Meyners, D., Quandt, E., Wagner, B. and Lofink, F., "AlScN-based MEMS magnetoelectric sensor," Appl. Phys. Lett. **117**(13), 132903 (2020).
[20] Zhu, S., Zhong, Q., Li, N., Hu, T., Dong, Y., Xu, Z., Zhou, Y., Fu, Y. H. and Singh, N., "Integrated ScAlN Photonic Circuits on Silicon Substrate," Conference on Lasers and Electro-Optics, STu3P.5, Optical Society of America, Washington, DC (2020).
[21] Bian, K., Li, Z., Zhao, X., Qiu, Y., Zheng, S., Dong, Y., Zhong, O. and Hu, T., "Integrated Scandium-Doped Aluminum Nitride Microring Resonators on 8-Inch Silicon Wafers," 2023 Asia Communications and Photonics Conference/2023 International Photonics and Optoelectronics Meetings (ACP/POEM), 1–5 (2023).
[22] Xin, M., Li, N., Singh, N., Ruocco, A., Su, Z., Magden, E. S., Notaros, J., Vermeulen, D., Ippen, E. P., Watts, M. R. and Kärtner, F. X., "Optical frequency synthesizer with an integrated erbium tunable laser," Light Sci. Appl. **8**(1), 122 (2019).
[23] Li, N., Su, Z., Purnawirman, Salih Magden, E., Poulton, C. V., Ruocco, A., Singh, N., Byrd, M. J., Bradley, J. D. B., Leake, G. and Watts, M. R., "Athermal synchronization of laser source with WDM filter in a silicon photonics platform," Appl. Phys. Lett. **110**(21), 211105 (2017).
[24] Sun, J., Kumar, R., Sakib, M., Driscoll, J. B., Jayatilleka, H. and Rong, H., "A 128 Gb/s PAM4 Silicon Microring Modulator With Integrated Thermo-Optic Resonance Tuning," J. Light. Technol. **37**(1), 110–115 (2019).
[25] Rosenberg, J. C., Green, W. M. J., Assefa, S., Gill, D. M., Barwicz, T., Yang, M., Shank, S. M. and Vlasov, Y. A., "A 25 Gbps silicon microring modulator based on an interleaved junction," Opt. Express, **20**(24), 26411–26423 (2012).
[26] Li, N., Chen, G., Lim, L. W., Ho, C. P., Xue, J., Fu, Y. H. and Lee, L. Y. T., "Fully integrated electrically driven optical frequency comb at communication wavelength," Nanophotonics **11**(13), 2989–3006 (2022).
[27] Stern, B., Ji, X., Okawachi, Y., Gaeta, A. L. and Lipson, M., "Battery-operated integrated frequency comb generator," Nature **562**(7727), 401–405 (2018).